JOURNAL OF SOLID STATE CHEMISTRY 73, 127–139 (1988)

Infrared and Raman Spectroscopies of rf Sputtered Tungsten Oxide Films

M. F. DANIEL, B. DESBAT, AND J. C. LASSEGUES*

Laboratoire de Spectroscopie Moléculaire et Cristalline, UA 124 CNRS, Université de Bordeaux I, 351, Cours de la Libération, 33405 Talence Cedex, France

AND R. GARIE

Laboratoire d'Etude des Matériaux pour la Microélectronique, Université de Bordeaux I, 351, Cours de la Libération 33405, Talence Cedex, France

Received February 25, 1987; in revised form June 22, 1987

Infrared and Raman spectroscopies have been applied to study rf sputtered tungsten oxide films as prepared and after the chemical modifications induced by successive coloration/bleaching cycles. As seen from UV–visible spectra and X-ray diffraction patterns, these films remain essentially amorphous, but it is shown that infrared spectroscopy used in absorbance and reflectance modes and with *s* and *p* polarized light is particularly well adapted to provide new information about their aging and variation of composition during the cycles. Aging effects are characterized by water adsorption and hydroxyl group formation. The modification of the amorphous initial film after annealing has also been investigated. The infrared spectra of the film after coloration or bleaching in a sulfuric acid solution show the important role of water content equilibration during the first coloration and then the reversible water extraction/injection during the following bleaching/coloration cycles. The structure of the colored film is also characterized by W=O terminal groups which disappear in the bleached state. Some coloration/bleaching cycles have also been performed in organic electrolytes for comparison.

Introduction

A huge amount of work has been devoted to the preparation of tungsten oxide films, to the study of their structural and electrical properties, and to their application in electrochromic (or electrochemichromic) devices (*1*). In fact, the research on display devices, sometimes based on rather empirical rules, seems to have progressed faster than the understanding of the mechanism of coloration/bleaching itself.

Although it is now well established that the blue coloration in a system electrode/WO_3/electrolyte/counter electrode occurs by combined injection of electrons and small cations (H^+, Li^+, Na^+, . . .), a number of problems subsist. Which are exactly the structural and electronic changes induced by the electron and cation accommodation? The intervalence charge-transfer mechanism proposed by Faughnan *et al.*

* To whom correspondence should be addressed.

0022-4596/88 $3.00

(*2*) seems to be generally accepted: the electron injected from the electrode would be trapped at a W^{6+} site to give a W^{5+} colored center and the light absorption would occur by charge transfer between two adjacent tungsten ions according to

$$W_A^{5+} + W_B^{6+} + h\nu \rightleftarrows W_A^{6+} + W_B^{5+} \quad (1)$$

The electronic levels involved in this process have even been deduced from XPS (*3*) and ESR (*4*) measurements.

However, other models have been suggested, for example, the small polaron (*5*) for which electrons injected into WO_3 are trapped at tungsten sites to form W^{5+} centers. They perturb the surrounding lattice and form small polarons. The optical transfer of the polaron also occurs from a W^{5+} site to a neighboring W^{6+} site. In the case of crystallized samples a different model is invoked (*5, 6*). The conduction there is explained by a free electron model of Drude type. Furthermore, it is not obvious whether a unified description can be applied to the large variety of materials produced by methods as different as thermal evaporation, radiofrequency reactive sputtering, anodic oxidation, etc.

On the other hand, the role of the cation injected from the electrolyte is not fully assessed. Does it serve only in local charge compensation or is it also involved in a decisive structural change around the W^{5+} center?

The more general opinion is that water plays an important role (*7*) and that cations are effectively inserted and extracted reversibly during the coloration/bleaching process (*2*).

This can be summarized by the reaction scheme proposed by Lusis *et al.* (*8*),

$$WO_{3-y} \cdot mH_2O + xH^+ + xe^- \leftrightarrows H_xWO_{3-y} \cdot mH_2O$$

or

$$W_x^{5+}W_{1-x}^{6+}O_{3-y}^{2-}(H_3^+O)_x(H_2O)_{m-x} \quad (2)$$

However, other authors claim that, after the first coloration/bleaching cycle, there is no further cation injection from the electrolyte but only internal rearrangement in M_xWO_3 (*9*).

By reading all the literature on this subject, one realizes that direct experimental proof of the cation injection/extraction is indeed rather scarce. In the case where the electrolyte is a liquid or a solid protonic conductor ($M^+ = H^+$ or H_3O^+), infrared (IR) spectroscopy seems to be a well-adapted technique to follow the coloration/bleaching process, due to its high sensitivity to the presence of OH groups of any kind.

Raman spectroscopy plays a complementary role by its sensitivity to structural changes via the generally narrower and intense vibrational lines of the W–O skeleton observed below 1000 cm^{-1}. This latter technique has been applied rather extensively (*10, 11*), particularly by Pham Thi and Velasco (*10*), to the characterization of WO_3 films on various substrates but the former has been little used or has given spectra of relatively poor quality.

In a previous publication, we have analyzed the IR and Raman spectra of monoclinic and hexagonal WO_3 and of the hydrates WO_3, xH_2O ($x = 1, 2, \frac{1}{3}$) (*12*). The aim of the present work is to see whether vibrational spectroscopy, and particularly infrared, can provide complementary information for an understanding of coloration/bleaching in thin tungsten oxide films.

Experimental Conditions and Preliminary Characterization of the Sputtered Tungsten Oxide Films

Thin tungsten oxide films have been prepared by rf reactive sputtering from a metallic tungsten target in a pure oxygen atmosphere or in a gaseous mixture of 20% oxygen in argon. After the chamber has been evacuated to $\sim 10^{-6}$ Torr, the gases

were introduced at a rate of 0.035 liter/min up to a pressure of 3×10^{-2} Torr.

The rf power was 32 W corresponding to a target voltage of 160 V. The water-cooled substrate was kept 5 cm from the target. Under these conditions, a sputtering time of 3 hr was generally used to produce film thicknesses of about 1500 Å in pure O_2 and 2200 Å in O_2–Ar.

The substrate was silicon, aluminium, glass, alumina, or graphite depending of the kind of analysis to be performed, respectively, IR transmission, IR reflection or Raman, visible absorption, X-ray diffraction, or Rutherford back-scattering (RBS).

The film thickness and stoichiometry were evaluated from this latter technique with a precision of the order of 5%. The 1500-Å film produced in pure O_2 was found to have a ratio [O]/[W] of 3.20 just after sputtering, and one of 3.28 after a few days. For the 2200-Å film produced in O_2–Ar, [O]/[W] = 3.10 after sputtering, 3.18 after about 10 days, and up to 3.28 after several months. We never tried in this process to avoid exposure of the sample to ambient air, i.e., hydration of the film, because the presence of water is a rather favorable factor for the electrochromic properties (*13*). The initial high value of 3.10 even suggests that residual water is present in the chamber. In previous sputtering preparations substoichiometric WO_{3-y} films with $y \sim 0.1$ to 0.2 are reported (*9, 14*).

Our sample seems to correspond to the general formula WO_{3-y}, mH_2O with $3 - y + m > 3$. However, for simplicity we will refer it as WO_3 in the following.

As a preliminary characterization, we have recorded optical absorption spectra between 300 and 2000 nm with a Cary 17 spectrometer. They are reported in Fig. 1 and allow us to check the similarity between the coloration/bleaching optical properties of our sample and those reported previously in the literature (*2, 5, 15*). In particular, the colored state is characterized by a strong absorption at about 900 nm (1.38 eV) and an optical gap E_g of 3.1 eV is deduced for the bleached state from an $(\alpha\hbar\omega)^{1/2} = f(\hbar\omega)$ plot, where α is the absorption coefficient.

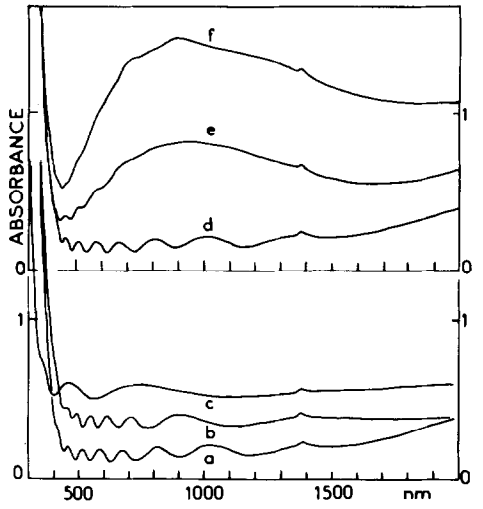

FIG. 1. Optical absorption of tungsten oxide sputtered on a glass substrate. (a) Initial deposit WO_3/ITO/glass, (b) ITO/glass, (c) WO_3/glass, (d) WO_3/ITO/glass after coloration and bleaching with +1.5 V, (e) WO_3/ITO/glass coloration with −1. V, (f) WO_3/ITO/glass after coloration with −1.5 V. Spectra (b) and (c) have been translated upward respectively by +0.2 and +0.4 in absorbance for comparison with (a). The spectra of the bleached state (d) are identical with that of the initial deposit (a).

It must be pointed out that no significant spectral differences are detected between the pure O_2 and the O_2–Ar preparations.

X-ray diffraction using a powder diffractometer with Cu$K\alpha_1$ line (λ = 1.54 Å) shows that the initial deposits on alumina are amorphous. Annealing at 693 K for 30 min gives a diffraction pattern corresponding to a symmetry very close to orthorhombic although similar patterns are sometimes indexed in the triclinic symmetry (*16*).

In all the experiments where the colored and bleached states were studied (IR and visible absorption, Raman), we have used a 1 *N* H_2SO_4 solution as electrolyte. In the case where the substrate was conductor (al-

uminium, doped silicon), it was used as electrode whereas glass was coated with ITO by rf sputtering from a 10% SnO_2, 90% In_2O_3 target. The counterelectrode was a platinum plate.

The IR spectra were recorded between 4000 and 200 cm^{-1} on a Perkin–Elmer 983 G spectrometer with an average resolution of 5 cm^{-1}. Transmission experiments were performed under normal or oblique incidence from WO_3 deposited on a piece of silicon wafer. Reflection experiments were performed with a Eurolabo accessory allowing the incidence angle to be varied between ~12 and 80°. The WO_3 was then deposited on an aluminium thin plate.

In the two kinds of experiments, the incident light was sometimes polarized either in the incidence plane (p) or perpendicular to it (s).

The Raman spectra were recorded with a Coderg T 800 or a Ramanor Jobin et Yvon spectrometer equipped with an ionized argon laser (λ_0 = 488.0 or 514.5 nm).

Rather large slit widths (resolution ~10 cm^{-1}) were used in order to keep the laser at the minimum power and to avoid local annealing or decoloration of the film deposited on aluminium. The incident light made an angle of about 80° with the surface held vertically.

Results

No significant differences have been observed between the vibrational spectra of WO_3 prepared in pure O_2 or in O_2–Ar. So we report only the results obtained for the latter which proved to present slightly better electrochromic properties.

1. Aging of a Film in Ambient Air

We have reported in Fig. 2a the IR spectra of tungsten oxide just after sputtering on silicon, but without avoiding exposure to ambient air during the transfer to the spectrometer. Aging has already started as indicated by water absorptions at 3300 and 1620 cm^{-1}. The amorphous character of the film is indicated by the presence of only two broad absorptions with maxima at ~650 and ~300 cm^{-1}.

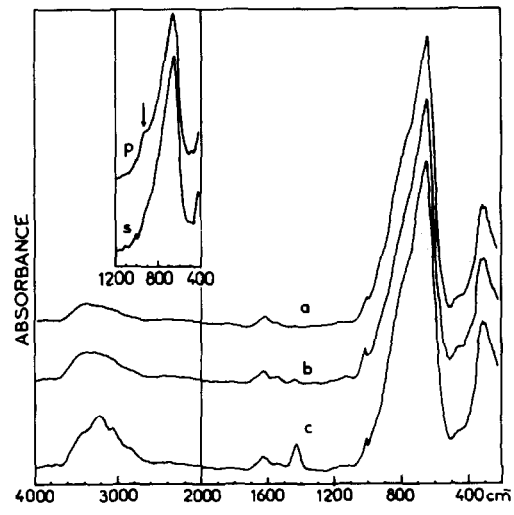

FIG. 2. IR spectra of a WO_3 film (~2200 Å) sputtered on silicon after subtraction of the silicon background and baseline correction. (a) Just after sputtering; (b) after a few hours exposure to the atmosphere; (c) after 1 month of aging. The profile of the main absorption band taken under oblique incidence (~45°) and polarized light is given in the insert.

By further exposure to the atmosphere, a two-step aging process seems to occur. After a few hours, the two water absorptions have increased in intensity. The bands due to the W–O vibrations are unchanged, although a weak absorption at 1015 cm^{-1} is now better defined (Fig. 2b).

After several days, a new absorption appears at 1425 cm^{-1} and the high-frequency ν(OH) band splits into three components at 3440, 3220, and 3050 cm^{-1} (Fig. 2c).

This is the final stage of evolution of these films as shown by spectra taken several months after preparation. X-ray diffraction has confirmed their amorphous nature; however, some degree of local order seems to subsist. In the insert in Fig. 2, we have reported the profile of the main W–O band between 400 and 1200 cm^{-1} recorded

under oblique incidence and with polarized light. For the *p* polarization which provides an electric field component normal to the surface, a new absorption appears at 960 cm^{-1}.

A similar WO_3 deposit on aluminium has also been studied by IR specular reflection several days after sputtering. The incidence angle has been varied between 20 and 75° and the two extreme situations are reported in Fig. 3 with *p* and *s* polarized light. Drastic spectral modifications are observed as a function of the incidence angle and the polarization.

At 20° (Fig. 3a) the ν(OH) absorptions dominate the spectrum and the 1620- and 1425-cm^{-1} bands are still well detected. The absorption profiles corresponding to the vibrations of the W–O–W framework between 1000 and 200 cm^{-1} are much weaker.

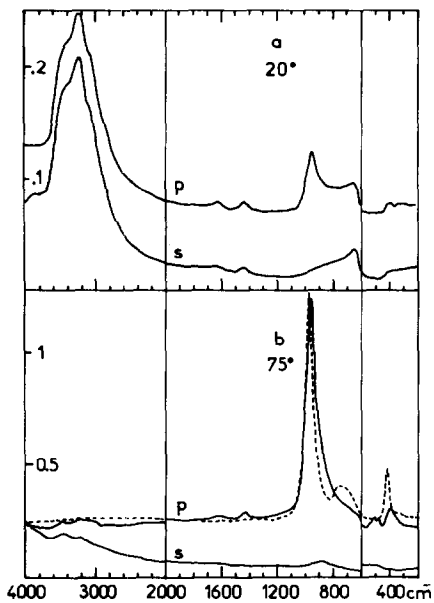

FIG. 3. IR spectra reflection with polarized light from a WO_3 film sputtered on aluminum, angle of incidence (a) 20°, (b) 75°. The dotted line represents the spectrum obtained after heating the film at 693 K for 30 min. The ordinate scale corresponds to $-\log(R/R_0)$, where R is the reflectance of the sample and R_0 that of a reference mirror. The spectra are shifted for convenience but have the same amplification in each series.

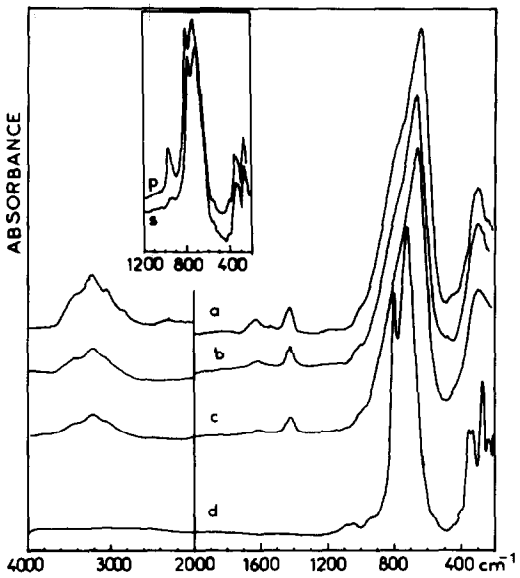

FIG. 4. IR spectra of WO_3 sputtered on silicon after subtraction of the silicon background and baseline correction. (a) Initial deposit at room temperature; (b) after annealing at 413 K; (c) after annealing at 493 K; (d) after annealing at 693 K. In this latter case, the main absorption band recorded under oblique incidence (~45°) and polarized light is given in the inset. Each annealing was performed for about 30 min.

In the *s* polarization, the main band resembles that observed in absorption (Fig. 2c) but in the *p* polarization a new component shows up at 955 cm^{-1}.

At 75° (Fig. 3b), this latter band is by far the more intense in the *p* polarization. The spectrum in the *s* polarization plotted on the same intensity scale is nearly flat. All these spectra have been taken with reference to a mirror.

2. Annealing Effects on an Aged Film

The spectra reported in Fig. 4 are recorded at room temperature but after various thermal treatments. It can be seen that annealing at 413 and 493 K leaves the W–O bands nearly unchanged whereas the OH band intensities decrease progressively. One can note the faster decrease in the 1620-cm^{-1} absorption relative to the 1425-cm^{-1} absorption.

After annealing at 693 K, the spectrum is strongly modified. All the absorptions above 1200 cm^{-1} have disappeared and the main bands at 650 and ~300 cm^{-1} become structured as expected from the crystallization of the sample. Maxima appear at 800, 720, 350, 325, and 270 cm^{-1}.

Furthermore, as shown in the insert in Fig. 4, this partially crystallized sample studied under oblique incidence and polarized light gives an additional band at 970 cm^{-1} in the *p* polarization. This band is much better defined than that of the initial deposit (Fig. 2).

3. *Coloration/Bleaching*

Several experiments have been performed on various deposits and at different times in order to ensure the reproducibility of the phenomena. A given experiment is performed during the same day, without interruption between the coloring and the bleaching operations other than the time interval needed to apply the required voltage in sulfuric acid, to wash the sample with acetone, and to dry it.

a. Infrared spectra. We show in Fig. 5 the direct spectra of the silicon background and of bleached and colored WO_3 on silicon in order to emphasize the strong variations in transmission which occur among the three samples as a result of absorption and reflection (diffuse and specular).

The silicon wafer has a mean transmission level of 32% instead of about 50% because it is polished only on one side.

It has been chosen for its resistivity of about 1 Ω/cm which allows it to be used as electrode in the coloration/bleaching process. Oxygen is the main dopant as shown by the 1100-cm^{-1} ν(Si–O) band which is nearly as intense as the intrinsic silicon absorptions around 600 cm^{-1} (Fig. 5a).

The initial and bleached films on silicon have about the same level of transmission as the bare silicon itself because the losses by reflection are roughly the same in both

FIG. 5. Transmission spectra as recorded of (a) the silicon substrate, (b) bleached WO_3 on silicon, and (c) colored WO_3 on silicon.

cases. Thus the silicon background can be subtracted rather precisely to give an absorbance spectrum with a baseline close to zero (Fig. 6a). When the film is colored, the transmission level is much lower than that for silicon and presents a negative slope toward high frequencies as expected from its metallic character. The subtracted spectrum (Fig. 6b) is then composed of absorption above the dotted line and of a high level of reflection below this line.

It is well known that a quantitative evaluation of these effects needs a complete treatment of the multireflections and absorptions in the film and in the substrate taking into account the huge variations of the film optical constants between the bleached and the colored states (*17*). However, for a qualitative description of the coloration/bleaching process, we have simply applied a baseline correction to substracted spectra of the kind represented in Fig. 6. In addition, we have expanded in Fig. 7 the 1800- to 900-cm^{-1} spectral range where the more interesting modifications occur. In-

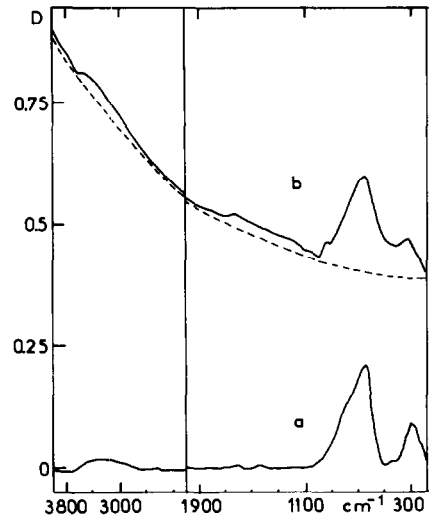

FIG. 6. Infrared spectra in absorbance resulting from the subtractions (a) 5b − 5a, and (b) 5c − 5a.

deed, it would be difficult to deduce any detailed information from the broadening and intensification of the ν(OH) profile between 2500 and 3700 cm^{-1} which are observed at the coloration. On the other hand, the stretching and bending modes of the W–O–W skeleton below 900 cm^{-1} do not exhibit significant changes.

The more striking modifications at the first coloration are an increase in the 1620-cm^{-1} band, a decrease in the 1425-cm^{-1} band, and the appearance of a new absorption at 950 cm^{-1} (Fig. 7b). After the first bleaching (Fig. 7c) a spectrum similar to the initial one is recovered but with slightly different intensities for the 1620- and 1425-cm^{-1} bands. The second coloration and bleaching do not bring further modifications compared to the first one. Bad adherence of the film on the silicon substrate and corrosion by sulfuric acid prevent a large number of cycles from being performed while keeping an acceptable basis of quantitative comparison between the spectra. However, it is observed qualitatively that the colored and bleached states present henceforth the characteristic spectral profiles given in Figs. 7d and 7e.

We show in Fig. 8 the variation of the 950-, 1620-, and 1425-cm^{-1} band intensities during the cycles.

It is very important to note that these observations have been made on various films either just after sputtering or after aging and they were prepared either in pure oxygen or in argon–oxygen atmospheres. As described above, their initial spectra differ by the intensity of the 1620- and 1425-cm^{-1} bands and by the presence of a more or less well-defined weak absorption at 1015 cm^{-1}. In all cases, the coloration produces an increase in the 1620-cm^{-1} band and the appearance of the 950-cm^{-1} absorption. This is true even when the 1015-cm^{-1} weak fea-

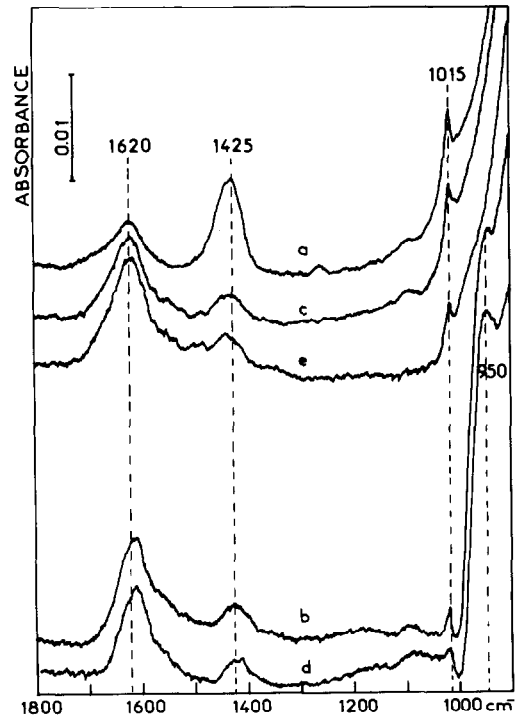

FIG. 7. IR spectra of a coloration/bleaching cycle. (a) Initial deposit (identical to that of Fig. 2c); (b) first coloration; (c) first bleaching; (d) second coloration; (e) second bleaching. A baseline correction has been applied to all spectra.

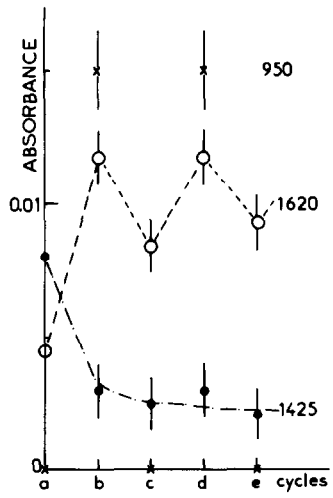

FIG. 8. Intensity at the maximum of the 950-, 1620-, and 1425-cm^{-1} bands during the coloration/bleaching process (see Fig. 7).

ture is not initially present (Fig. 6). Therefore one can clearly exclude any kind of exchange between species associated with the 950/1015-cm^{-1} bands at the coloration/bleaching. One can remark in Fig. 7 that the latter tends simply to disappear during the cycles.

Further confirmation of the generality of these observations is provided by the study of films produced by evaporation of solid WO_3 or of colloidal tungsten oxide. These amorphous films were more hydrated than the sputtered ones but a new band at 950 cm^{-1} also appeared at the coloration. Finally, other coloration/bleaching experiments have been performed using anhydrous electrolytes such as NH_4SCN/CH_3OH and $LiI/(CH_3)_2CO$. The spectra reported in Fig. 9 show that with increasing voltage at the coloration, not only does the reflectivity increase, as expected, but the bands at 1420 and 950 cm^{-1} also increase with NH_4SCN. In the case of $LiI/(CH_3)_2CO$ as electrolyte, the 950-cm^{-1} band appears only as a shoulder.

b. Raman spectra. We have only recorded the Raman spectra of a bleached and colored film deposited on aluminium for comparison with the IR data and with the rather extensive studies performed previously by Pham Thi *et al.* (*10*) on sputtered WO_3 and by Delichere *et al.* (*11*) on anodic WO_3.

The Raman spectra (Fig. 10) are only reported below 1200 cm^{-1} as no signal could be detected above.

The bleached state is characterized by three broad bands centered at about 950, 770, and 280 cm^{-1} (Fig. 10a). This profile is modified in the colored state essentially by an increase in the 950-cm^{-1} component (Fig. 10c). This is a reversible process but it must be pointed out, in addition, that the colored state is very sensitive to the laser as shown by a fast evolution of its spectrum toward that of the bleached state at a laser power of ~100 mV (Fig. 10b).

The Raman spectrum of an annealed film (same specimen as that used in the IR reflection experiment (Fig. 3b)) has been re-

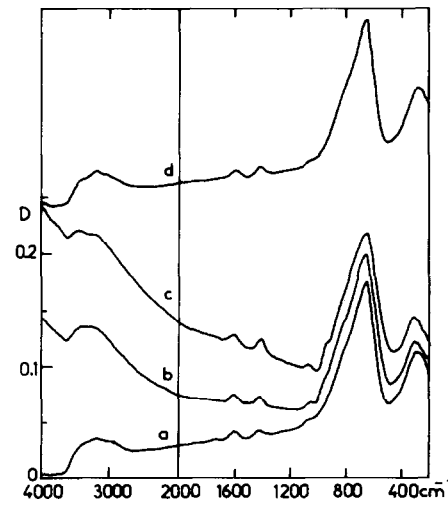

FIG. 9. IR spectra of a WO_3 film deposited on silicon and colored/bleached with an NH_4SCN/CH_3OH electrolyte: (a) initial film, (b) colored with 6 V, (c) colored with 12 V, (d) bleached. The intensity scale applies only to spectrum (a). The other spectra are shifted for convenience but have been recorded under the same expansion conditions.

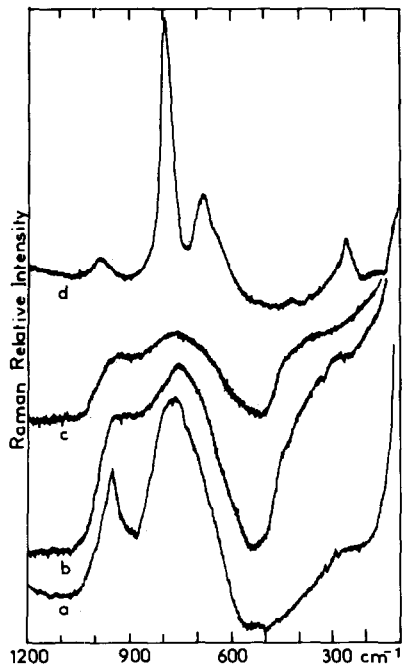

FIG. 10. Raman spectra of WO_3 deposited on aluminium (a) as prepared or bleached, (b) after coloration and prolonged exposure to the laser, (c) just after coloration, (d) of the initial deposit in the HH polarization after annealing at 693 K for 30 min.

ported for comparison. At the difference between the amorphous deposits which were studied without polarization analysis, we have recorded the spectra of the annealed film under the VV, VH, HV, and HH geometries. The first letter V (vertical) or H (horizontal) indicates the state of polarization of the incident laser and the second letter that of the scattered electric field. We have only reported the HH spectrum in Fig. 10d. The other spectra have a similar shape with band maxima at 970, 800, 680, and 270 cm^{-1}. Differences only occur in the global intensity of this pattern of lines: the HH spectrum is three times more intense than the VH one and the HV and VV spectra have intermediate intensities.

It can be noted that this kind of spectrum, very different from those of the bleached and colored states (Figs. 10a–10c), resembles now those of the monoclinic and hexagonal forms (*12*).

Discussion

1. Initial Tungsten Oxide Films

It is convenient to consider first the films annealed at 693 K because they are completely free from water and are very similar in composition and structure to well-known crystallographic modifications of WO_3 as indicated by X-ray diffraction. The infrared (Fig. 4d) and Raman (Fig. 10d) spectra present effectively well-defined and relatively narrow bands at frequencies which are very similar to those of monoclinic (or triclinic) WO_3, although it is not possible from these spectra to distinguish between orthorhombic, triclinic, or monoclinic modifications. The main IR absorptions at 800, 720, 350, 325, and 270 cm^{-1} (Fig. 4d) have very different intensities in Raman but have similar frequencies (800, 680, 270 cm^{-1}) (Fig. 10d). All these values are in good agreement with those found for monoclinic tungsten trioxide (m–WO_3) (*12*). However, an unexpected Raman line occurs at 970 cm^{-1} (Fig. 10d) and the band shape and intensities are very different from those of m–WO_3 especially in the infrared. This can be due to the very different grain sizes of the two samples and/or to partially anisotropic crystallization of the film, but the conditions of observation are different. In particular, the Raman spectra of the film are taken under oblique incidence. As recalled in a recent publication (*18*), complex polarization effects can occur according to the scattering geometry and this must be kept in mind for a comparison of literature Raman results obtained from thin WO_3 films under different conditions. Thus, the 970-cm^{-1} Raman line is assigned to a longitudinal optic (LO) mode of the W–O bond. Indeed, it cannot be due to terminal W=O oscillators which have no reason to exist in

such annealed WO_3 films and should be detected in the transmission IR spectra (Fig. 4d). On the other hand, a new band appears at 975 cm^{-1} in the IR reflection spectra under *p* polarization (Fig. 3) or at 970 cm^{-1} in the transmission spectra under oblique incidence (Fig. 4). The specificity of these particular geometries is to provide an electric field component perpendicular to the surface and thus to excite LO modes. This is particularly true for the IR reflection experiment at 75° with *p* polarization which is close to the conditions defined by Greenler (*19, 20*) for the optimal detection of a thin film on a metal substrate. Indeed, at high incidence angles, a great standing wave amplitude is achieved at the location of the absorbing layer. One can see from Fig. 3b that the high intensity observed for a 2200-Å WO_3 layer on aluminium would allow one to obtain a measurable signal even for a 20 times thinner film. But it must again be emphasized that this kind of spectrum reveals essentially LO excitations.

In the case of amorphous deposits, the main LO mode is still well detected. One simply notes a shift of its maximum to 955 cm^{-1} (Fig. 3b). It is also observed under oblique incidence (Fig. 2) and we believe that it also contributes strongly to the intensity of the Raman line at 950 cm^{-1} (Fig. 10a).

Thus, it is very important for the following to take into consideration that the infrared reflection and oblique transmission spectra and the Raman spectra exhibit between 950 and 975 cm^{-1} a LO mode, more or less well defined according to the more or less crystallized state of the sample. The corresponding TO mode can be located only near 800 cm^{-1} where W–O stretching motions of the W–O–W framework are mainly involved (*12*).

As already pointed out, the presence of –OH groups is easily detected in the IR spectra; for initial WO_3 films, the high-frequency broad absorption at ~3300 cm^{-1} and the 1620-cm^{-1} band (Fig. 2a) are assigned respectively to ν(OH) and δ(OH) modes of absorbed water. The 1425-cm^{-1} band which appears by exposure to ambient air, as for WO_3, $\frac{1}{3}H_2O$ (*12*), is assigned to δ(OH) of a W–O–H group.

The ν(OH) vibration of this group is certainly responsible of the structuring of the high-frequency band (Fig. 2c) and again, by comparison with WO_3, $\frac{1}{3}H_2O$, it can be situated at 3220 cm^{-1}. These frequencies are rather unusual for a hydroxyl group. The stretching and bending modes are generally observed respectively at higher and lower frequencies (*12*). Thus, the δ(OH) vibration in tungsten bronzes $H_{0.4}WO_3$ has been situated at 1146 cm^{-1} (*21*). The present W–O–H group is certainly rather strongly hydrogen bonded to further adsorbed water molecules or even to surface oxygen atoms.

Little information must be found in the profiles of the stretching and bending vibrations of the W–O–W framework which are centered respectively at ~650 and 300 cm^{-1} and remain broad for the "as prepared" amorphous deposit. The corresponding Raman bands are centered at ~770 and 280 cm^{-1} and are also very broad. It is thus difficult to deduce any significance structural information by comparison with the spectra of WO_3 and WO_3, xH_2O.

The aging effect represented in Fig. 2 seems to involve two steps. The amount of adsorbed water first increases. The characteristic frequencies of these water molecules indicate that they are physisorbed at the surface and in the pores of the structure rather than engaged in a $W–OH_2$ bond as in the hydrates WO_3, xH_2O. In this latter case a characteristic terminal W=O bond would indeed be found at ~950 cm^{-1} (*12*).

However, we have seen that the Raman spectrum of the initial deposit presents an intense and well-defined line at 950 cm^{-1}. We have varied the incident laser wavelength to see whether some resonance effect was responsible for the intensification

of W=O terminal oscillators even in small quantities and undetected by IR. The profile does not change with λ_0 = 514.5 or 488.0 nm. So, following the arguments developed above in the analysis of the IR spectra under *p* polarization and after annealing, we are tempted to assign the 950-cm^{-1} Raman line essentially to the LO mode which has unfortunately about the same frequency as a terminal W=O stretching vibration.

The second step of aging seems to correspond to a partial reaction of water with tungsten oxide by hydroxylation and/or hydrolysis as postulated by Yoshiike and Kondo (*22*).

These authors propose two reaction schemes

$$—O—W=O + H_2O \rightarrow —O—W(OH)—OH$$

$$O—W—O—W—O + H_2O \rightarrow O—W—OH + HO—W—O$$

As rather few terminal W=O groups are available and since the surface W=O groups giving the 1015-cm^{-1} band subsist, we prefer the second kind of reactions to explain the occurrence of hydroxyl groups and deduce from their characteristic frequencies that they are not free but engaged in a $—O—W—OH \ldots O<^{H}_{H}$ type of complex.

Actually, two interpretations are possible for the small peak observed at 1015 cm^{-1}. It could be due either to terminal W=O groups formed at the surface of the film or to W=O groups coordinated to the Si (or SiO_2) surface by analogy with previous observations on very thin WO_3 films on TiO_2 or Al_2O_3 substrates (*23*). However, it must be recalled that even if the shape and intensity of this 1015-cm^{-1} band vary from one sample to another, it always remains very weak compared to the other spectral features. Thus the corresponding oscillator does not seem to play an important role in the electrochromic properties of tungsten oxide.

2. *Coloration/Bleaching*

The coloration/bleaching cycles are characterized by several major spectroscopic features in the mean infrared:

(a) The blue coloration corresponds to a strongly increased electronic conductivity of the film (*24*) and this metallic character explains the very important differences between the reflectivities of the bleached and colored states.

(b) The hydroxyl groups present in the initial deposit disappear during the cycles but the amount of water, measured on the 1620-cm^{-1} band, first increases by coloration and then oscillates, in agreement with the hypothesis of insertion/extraction during the coloration/bleaching cycles.

The first coloration seems to have the important role of equilibration of the optimal water content in the film and (accessorially) of destruction or transformation of the hydroxyl groups and W=O surface groups.

(c) A new band appears by coloration at 950 cm^{-1} and disappears by bleaching. Since it is observed in normal transmission experiments, it can only be due to a TO mode and is definitely differentiated from a LO mode of the tungsten to oxygen bond which appears at nearly the same frequency under polarized reflection and oblique incidence. On the basis of previous literature data, this 950-cm^{-1} absorption band can confidently be assigned to W=O terminal groups involved in an arrangement similar to that for the hydrates WO_3, xH_2O (*12*).

(d) The Raman spectrum of the colored state (Fig. 10) also presents a strong intensification at ~950 cm^{-1} but it can be noted that the profile of this band is much broader than that in the bleached state. We think that terminal W=O groups are responsible of this intensification.

The experiments using NH_4SCN/CH_3OH and $LiI/(CH_3)_2CO$ as electrolytes confirm points (a) and (c). In the case of coloration with NH_4^+, the increase in the 1420-cm^{-1} band is associated with injection of this cation. Unfortunately, the deformation mode of NH_4^+ appears at the same frequency as the δ(OH) bending mode of W–O–H groups which were initially present in the deposit (Fig. 9). So a quantitative evaluation of NH_4^+ injection/extraction is difficult.

The shape of the more intense absorption bands due to the W–O–W framework vibrations is nearly the same in all cases preventing any detection of structural changes during the coloration/bleaching and/or as a function of the nature of the injected cation.

Thus, the more important conclusion remains to be the formation at the coloration of a local structure involving a terminal W=O group and, in the case of sulfuric acid as electrolyte, the injection of water molecules presumably under the protonated form $H^+(H_2O)_n$.

The amount of water involved in the whole process can be roughly estimated from the initial value of 3.28 for the [O]/[W] ratio and the intensity variations of the 1620-cm^{-1} IR band (Figs. 7 and 8).

The initial aged film would contain approximately 0.3 water molecule per WO_3 unit.

At the first coloration, the 1620-cm^{-1} band intensity increases by a factor of 2.5 partly by transformation of hydroxyl groups and partly by injection of hydrated protons, leading to the global composition WO_3, $0.75H_2O$. The first bleaching decreases this quantity by about 25% to give WO_3, $0.55H_2O$.

Then, 0.2 water molecule would be involved in the following cycles and this figure is in good agreement with the quantities of protons generally supposed to be extracted/injected (*25*).

The other conclusion of this very crude calculation is that the colored or bleached films contain intermediate amounts of water between those of the known WO_3, H_2O, and WO_3, $\frac{1}{3}H_2O$ hydrates in which the water molecules are directly linked to tungsten within $O{=}W{<}OH_2$ species (*12*). The absence of terminal W=O groups in the bleached state suggests that water is instead adsorbed by hydrogen bonding —O—W—O. . .H—O$\diagup^{H}$, whereas the 0.2 active molecules injected at the coloration seem to provoke the appartition of W=O groups. As these 0.2 molecules actually hold a positive charge (H^+), we suppose that W=O is then included in some kind of polytungstate anion.

At this stage, it would be tempting to associate the W^{5+} formation at a tungsten site by electron trapping to the previously discussed chemical modifications, but without further information, any model would be very speculative.

Resonance Raman experiments, on a colored film, are planned to see whether a particular vibrational mode is involved in the electronic transitions responsible for the coloration in this mixed valence system.

Conclusion

The vibrational spectra of sputtered tungsten oxide films provide some new information on the composition and aging of these films and on the reversible chemical modifications occurring at the coloration/bleaching.

The films as prepared are found to correspond to a composition WO_{3-y},mH_2O with

$m - y = 0.1$. Aging first increases the amount of adsorbed water and then produces W—O—H groups up to a limiting value of ~0.28 for $m - y$. The unusual values of 3220 and 1425 cm^{-1} suggested for the stretching ν(OH) and bending δ(OH) modes of W–O–H indicate that the OH group is not free but is rather strongly bonded to additional water molecules or to surface oxygen atoms.

For the amorphous initial deposit as well as for the annealed one, a LO mode is clearly evidenced respectively at 950 and 975 cm^{-1}. It is shown that reflection experiments at high incidence angles using p polarized light provide a high detectivity of these films deposited on aluminum as predicted by Greenler (*19*).

Coloration/bleaching cycles give very specific IR spectra which show a strong increase in the water content at the first coloration up to $m \sim 0.75$ and then a decrease to $m \sim 0.55$ at the first bleaching. In the following cycles, about 0.2 water molecules are injected and extracted. At the same time a W=O terminal group is reversibly formed and destroyed during the coloration/bleaching cycles.

Although it would be difficult to deduce from these first results a precise description of the chemical composition and local structure of the tungsten oxyde bronze formed at the coloration, we believe that IR spectroscopy has provided new information and is still open to new developments. In a following paper we will present similar results obtained on amorphous evaporated and colloidal tungsten oxyde and on the determination of the optical constants of bleached and colored films from transmission and reflection mean- and far-infrared spectra.

Acknowledgments

The authors are very grateful to Professor J.L Salardenne, who is at the basis of this work, for many fruitful discussions and to Doctor C. Sourisseau for critically reading the manuscript.

References

1. W. C. DAUTREMONT-SMITH, Displays **4,** 3 (1982).
2. B. W. FAUGHNAN, R. S. GRANDALL, AND P. M. HEYMAN, *RCA Rev.* **36,** 177 (1975).
3. P. GERARD, A. DENEUVILLE, G. HOLLINGER, AND TRAN MINH DUC, *J. Appl. Phys.* **48**(10), 4252 (1977).
4. J. V. GRABUSENOKS, P. D. CIKMACK, AND A. R. LUSIS, *Solid State Ionics* **14**(1), 25 (1984).
5. O. F. SCHIRMER, V. WITTWER, G. BAUR, AND G. BRANDT, *J. Electrochem. Soc.* **124**(5), 749 (1977).
6. D. H. MENDELSOHN AND R. B. GOLDNER, *J. Electrochem. Soc.* **131**(4), 857 (1984).
7. B. REICHMAN AND A. J. BARD, *J. Electrochem. Soc.* **126**(4), 583 (1979).
8. A. R. LUSIS, J. J. KLEPERIS, A. A. BRISHKA, AND E. V. PENTYUSH, *Solid State Ionics* **13,** 319 (1984).
9. P. GERARD, A. DENEUVILLE, AND R. COURTHS, *Thin Solid Films* **71,** 221(1980).
10. M. PHAM THI AND G. VELASCO, *Rev. Chim. Miner.* **22,** 195 (1985).
11. P. DELICHERE, P. FALARAS, AND A. HUGOT-LE GOFF, "Tenth International Conf. on Raman Spectroscopy" (W. L. Peticolas and B. Hudson, Eds.), pp. 6–15, Eugene, 1986.
12. M. F. DANIEL, B. DESBAT, J. C. LASSEGUES, B. GERAND, AND M. FIGLARZ, *J. Solid State Chem.* **67,** 235 (1987).
13. N. YOSHIIKE AND S. KONDO, *J. Electrochem. Soc.* **130**(11), 2283 (1983).
14. M. R. GOULDING AND C. B. THOMAS, *Thin Solid Films* **62,** 175 (1979).
15. A. DENEUVILLE AND P. GERARD, *J. Electron. Mater.* **7(4),** 559 (1978).
16. B. REICHMAN AND A. J. BARD, *J. Electrochem. Soc.* **126,** 2133 (1979).
17. O. S. HEAVENS, "Optical Prop. of Thin Solid Films," Academic Press, New York, 1955.
18. M. HARRAND, *J. Chem. Phys.* **85**(5), 2429 (1986).
19. R. G. GREENLER, *J. Chem. Phys.* **44**(1), 310 (1966).
20. R. G. GREENLER, *J. Chem. Phys.* **50**(5), 1963 (1969).
21. C. J. WRIGHT, *J. Solid State Chem.* **20,** 89 (1977).
22. N. YOSHIIKE AND S. KONDO, *J. Electrochem. Soc.* **131**(4), 809 (1984).
23. S. S. CHAN, I. E. WACHS, L. L. MURRELL, L. WANG, AND W. K. HALL, *J. Phys. Chem.* **88,** 5831 (1984).
24. R. S. GRANDALL AND B. W. FAUGHNAN, *Phys. Rev. Lett.* **39,** 232 (1977).
25. B. W. FAUGHNAN AND R. S. GRANDALL, *Appl. Phys. Lett.* **27,** 275 (1975).